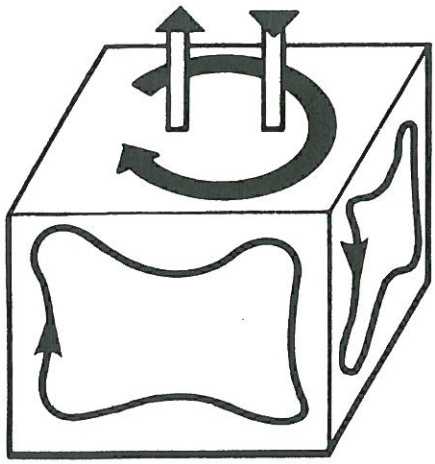

OCEAN modelling

ISSUE 101

DECEMBER 1993

FEATURING:

ON THE EDDY–POTENTIAL–ENSTROPHY BALANCE IN A TWO–LAYER QUASI–GEOSTROPHIC CHANNEL MODEL

J.-O. Wolff, A.V. Klepikov and D.J. Olbers

ABSTRACT

Computation of the eddy–potential–enstrophy (EPE) balance in a two-layer quasi-geostrophic eddy-resolving channel model with the well known second order Jacobian J_7 (Arakawa and Lamb, 1977) leads to artificial (numerical) correlations in terms of the EPE balance. It was shown by Arakawa that J_7 conserves mean energy, mean enstrophy and the property $J(q,\psi) = -J(\psi,q)$ and the experiments of McWilliams et al., (1978), Treguier and McWilliams (1990) and Wolff et al., (1991) have demonstrated that the numerical form of J_7 is sufficient to compute lower order statistics like the momentum balance. However, attempts to compute the EPE balance more or less failed or had curious results (see eg., McWilliams and Chow, 1981). A fourth order accurate formulation of the Jacobian (Arakawa, 1966) is necessary to compute this balance correctly.

INTRODUCTION

Results from quasi-geostrophic eddy-resolving models (e.g., McWilliams and Chow, 1981, Wolff et al., 1991) and analytical arguments (e.g., Marshall, 1981, Marshall and Shutts, 1981, Ivchenko, 1985) indicate, that a parametrization scheme for use in a low resolution ocean model based on eddy potential vorticity fluxes may lead to improved simulations. The coefficients of potential vorticity mixing appearing in these analytical models must be chosen correctly in terms of the magnitude and spatial variation, as shown by Marshall (1981) and Wolff et al., (1993), otherwise important dynamical constraints as the momentum balance will be violated. The balance equation for eddy potential enstrophy gives motivation to use down-gradient diffusive parametrizations of the eddy potential vorticity flux, it may also be used to determine the structure and magnitude of the diffusion coefficients. To test these ideas in an eddy–resolving numerical model it is necessary to diagnose a correct EPE balance. The simplest case is a flat bottom periodic channel, because in this case the mean advection of EPE has to vanish.

THE MODEL

The model used in this study is the one described in Wolff et al., (1991). For a more detailed description the interested reader is referred to the manual by Wolff (1993).

THE EDDY-POTENTIAL-ENSTROPHY (EPE) BALANCE

The potential vorticity balances in each layer

$$\frac{\partial q_i}{\partial t} + J(\psi_i, q_i) = F_i,\ i = 1,2 \qquad (1)$$

are averaged in time (indicated by an overbar) and than the time averaged equations are subtracted from (1) to give the eddy potential vorticity equations.

$$\frac{\partial q_i'}{\partial t} + J(\psi_i, q_i) - \overline{J(\psi_i, q_i)} = F_i',\ i = 1,2 \qquad (2)$$

Multiplying (2) with the eddy potential vorticity q' creates an equation for the EPE (dropping indices for clarity)

$$\frac{1}{2}\frac{\partial q'^2}{\partial t} + q'J(\psi,q) - q'\overline{J(\psi,q)} = q'F' \qquad (3)$$

Performing again a time average on (3) gives an expression for the mean EPE

$$\frac{1}{2}\overline{\frac{\partial q'^2}{\partial t}} + \overline{q'J(\psi,q)} - \overline{q'\overline{J(\psi,q)}} = \overline{q'F'} \qquad (4)$$

Assuming that the time averaging interval T is long enough to ensure that the time mean of the time derivative of the EPE vanishes (or is very small compared to the sum of all the other terms) and that the time mean of any perturbation is equal to zero we arrive at the balance equation for mean EPE

$$\overline{q'J(\bar{\psi},q')} + \overline{q'J(\psi',q')} + \overline{q'J(\psi',\bar{q})} = \overline{q'F'} \qquad (5)$$

In vector notation (underlined quantities indicate 2-dimensional vectors, e.g., $\underline{u} = (u,v)$) this is written as

$$\underline{\bar{u}} \cdot \underline{\nabla}\frac{1}{2}\overline{q'^2} + \underline{\nabla} \cdot \overline{\underline{u}'\frac{1}{2}q'^2} + \overline{\underline{u}'q'} \cdot \underline{\nabla}\bar{q} = \overline{q'F'} \qquad (6)$$

These terms describe the mean advection, redistribution, production and dissipation of EPE, respectively.

EPE IN A FLAT BOTTOM EXPERIMENT

Consider the possible solutions in a flat bottom experiment for very long time averaging in a quasi-stationary state:

$$\underline{\overline{u}} \equiv (\overline{u}, 0) \tag{7}$$

$$\underline{\nabla}\frac{1}{2}\overline{q'^2} \equiv (0, \frac{\partial}{\partial y}\frac{1}{2}\overline{q'^2}) \tag{8}$$

It follows that the scalar product of these two terms, the mean advection of EPE, must vanish because the vectors are orthogonal.

Furthermore the following holds

$$\underline{\nabla}\overline{q} \equiv (0, \frac{\partial}{\partial y}\overline{q}) \tag{9}$$

$$\underline{\nabla} \cdot \overline{\underline{u}'1/2q'^2} \equiv (0, \frac{\partial}{\partial y}\overline{v'1/2q'^2}) \tag{10}$$

and the mean EPE balances thus reads

$$\frac{\partial}{\partial y}\overline{v'1/2q'^2} + \overline{v'q'}\frac{\partial}{\partial y}\overline{q} = \overline{q'F'} \tag{11}$$

Here there is no zonal averaging involved, but because there is no zonal asymmetry in the forcing or topography, there can be no long term zonal asymmetry in the enstrophy terms.

NUMERICAL EVALUATION OF ENSTROPHY BALANCE

There are several ways to calculate the enstrophy balance. The following two ways have been used in this study

- Accumulated Statistics Run (ASR) : calculation of all terms in eq. (6) during the integration using the simplest direct centred differences (see below).
- "Real" Perturbations Run (RPR) : this consists of 2 long term integrations, where the first is used to compute stable mean fields and the second run repeats the first run, but directly uses perturbation fields and computes the EPE balance from eq. (5) using the same discretized Jacobian operator as in the time integration.

THE ACCUMULATED STATISTICS RUN (ASR) PROCEDURE

All necessary perturbation correlations can be computed during the time integration itself, i.e., it is not necessary to repeat a long integration in order to calculate the perturbation quantities. Consider the computation of the term

$\overline{q'^2}$.

$$\begin{aligned} \overline{q^2} &= \overline{(\overline{q}+q')(\overline{q}+q')} \\ &= \overline{q}\,\overline{q} + \overline{q'q'} \\ \Longrightarrow \overline{q'^2} &= \overline{q^2} - (\overline{q})^2 \end{aligned} \tag{12}$$

To obtain the eddy potential enstrophy we thus have to sum up the quantities $\overline{q^2}$ and $(\overline{q})$ over the length of the integration. At the end of the averaging period T one simply divides by the number of time steps N to reach time $T = N\Delta t$ and uses (7) to compute the perturbation correlation.

For the computation of the **mean advection of EPE**, the first term in eq. (6), we need in addition to $\overline{q^2}$ and $(\overline{q})$ the time mean fields of the velocity stream function $\overline{\psi}$ to calculate the time mean velocities.

$$\underline{\overline{u}} \cdot \underline{\nabla}\frac{1}{2}\overline{q'^2} = -\overline{\psi_y}\frac{1}{2}\overline{(q'^2)_x} + \overline{\psi_x}\frac{1}{2}\overline{(q'^2)_y} \tag{13}$$

Indices x and y denote partial derivatives. The second term in eq. (6), the **redistribution of EPE** is

$$\begin{aligned} \underline{\nabla} \cdot \overline{\underline{u}'1/2q'^2} &= \overline{(u'_x + v'_y)1/2q'^2} + \\ &\quad \overline{u'1/2(q'^2)_x} + \overline{v'1/2(q'^2)_y} && (14) \\ &= \overline{u'1/2(q'^2)_x} + \overline{v'1/2(q'^2)_y} && (15) \end{aligned}$$

because the perturbation velocity field has no divergence. So from

$$\begin{aligned} \overline{u(q^2)_x} &= \overline{(\overline{u}+u')\cdot(\overline{q}^2 + 2\overline{q}q' + q'^2)_x} && (16) \\ &= \overline{u}(\overline{q}^2)_x + \overline{u}\overline{(q'^2)_x} \\ &+ \overline{u'(2\overline{q}q')_x} + \overline{u'(q'^2)_x} && (17) \end{aligned}$$

$$\begin{aligned} \Longrightarrow \overline{u'\frac{1}{2}(q'^2)_x} &= \frac{1}{2}[\overline{u(q^2)_x} - \overline{u}(\overline{q}^2)_x - \overline{u}\overline{(q'^2)_x} \\ &\quad - 2\overline{q}_x\overline{u'q'} - 2\overline{q}\overline{u'q'_x}] \end{aligned} \tag{18}$$

we need

$$\overline{u'q'} = \overline{uq} - \overline{u}\,\overline{q} \tag{19}$$

and

$$\overline{u'q'_x} = \overline{uq_x} - \overline{u}\,\overline{q_x} \tag{20}$$

The same considerations hold for $\overline{v'1/2(q'^2)_y}$. In summary

$$\begin{aligned} \underline{\nabla} \cdot \overline{\underline{u}'\frac{1}{2}q'^2} &= \frac{1}{2}[\overline{u(q^2)_x} - \overline{u}(\overline{q}^2)_x - \overline{u}(\overline{q^2} - \overline{q}^2)_x \\ &\quad - 2\overline{q}_x(\overline{uq} - \overline{u}\,\overline{q}) - 2\overline{q}(\overline{uq_x} - \overline{u}\,\overline{q_x})] \\ &\quad + \frac{1}{2}[\overline{v(q^2)_y} - \overline{v}(\overline{q}^2)_y - \overline{v}(\overline{q^2} - \overline{q}^2)_y \\ &\quad - 2\overline{q}_y(\overline{vq} - \overline{v}\,\overline{q}) - 2\overline{q}(\overline{vq_y} - \overline{v}\,\overline{q_y})] \end{aligned}$$

The third term in eq. (6), the **production of EPE**, results in

$$\overline{\underline{u}'q'} \cdot \underline{\nabla}\overline{q} = (\overline{uq} - \overline{u}\,\overline{q})(\overline{q})_x + (\overline{vq} - \overline{v}\,\overline{q})(\overline{q})_y \tag{21}$$

The right hand side of eq. (6), the **dissipation of EPE**, follows easily as

$$\overline{q'F'} = \overline{qF} - \overline{q}\,\overline{F} \tag{22}$$

In summary we need time averages of the following variables to compute the EPE balances at the end of any length of time average

$$\overline{q},\quad \overline{q^2},\quad \overline{\psi},\quad \overline{\psi_x q},\quad \overline{\psi_y q},\quad \overline{\psi_x q_y},\quad \overline{\psi_y q_x},$$

$$\overline{\psi_x (q^2)_y},\quad \overline{\psi_y (q^2)_x},\quad \overline{qF},\quad \overline{F}$$

Any further diagnostics might be computed in an analogous way.

DISCRETIZATIONS OF THE JACOBIAN OPERATOR

Before we discuss the results of the two above mentioned methods to compute the EPE balance we make a detour to discuss the numerical discretizations of the Jacobian as given by Arakawa (1966). We like to redefine Arakawa's original notation slightly due to an ambiguousness in the original paper. Equation numbers like (A36) refer to eq. (36) in Arakawa (1966). The superscripts + and × indicate the numerical discretization stencil.

$$J_1 = J^{++} \qquad (A36)$$

$$J_2 = J^{\times +} \qquad (A38)$$

$$J_3 = J^{+\times} \qquad (A37)$$

$$J_4 = J^{\times\times} \qquad (A39)$$

$$J_5 = J^{\times +} \qquad (A57)$$

$$J_6 = J^{+\times} \qquad (A58)$$

$$J_7 = 1/3\,[J_1 + J_2 + J_3] \qquad (23)$$

$$J_8 = 1/3\,[J_4 + J_5 + J_6] \qquad (24)$$

$$J_9 = 2J_7 - J_8 \qquad (25)$$

As was shown by Arakawa (1966) only the Jacobians J_7, J_8 and J_9 conserve mean kinetic energy, mean enstrophy and the property of the Jacobian $J(q,\psi) = -J(\psi,q)$. All Jacobians but J_9 are of second order accuracy. J_9 is a fourth order approximation of the Jacobian (see A60).

ACCUMULATED STATISTICS RUN (ASR) EXPERIMENTS

The flat bottom channel experiment was started from a restart point in quasi-stationary equilibrium (Case FB, see Wolff et al., 1991). We integrated the model from that point for a total of 55 years (240.000 time steps with $\Delta t = 2$ hours) and accumulated the perturbation correlations.

a) J_7 – Experiment

The Jacobian used in the advection routine in this first experiment is J_7 (as in McWilliams et al., 1978, McWilliams and Chow, 1981, Treguier and McWilliams, 1990, Treguier, pers. comm. and in Wolff et al., 1991).

After calculating the terms in eq. (6) using the simplest direct centered differences we zonally averaged the fields. Fig. 1 shows the EPE balance for this case. The mean advection term is small as expected, but there is a quite substantial error term in the balance. The redistribution of EPE is also very small. We have monitored the balance every 10 years and the changes in the terms were only minor, which led us to conclude, that even extremely long time integrations would not reduce the error.

b) J_9 – Experiment

We repeated the first experiment using the fourth order Jacobian J_9 in the advection routine. Fig. 2 shows the EPE balance for this second experiment. The redistribution term has now roughly the shape and magnitude of the missing term (the negative error) of the first experiment. Interestingly the dissipation term has now a local minimum at the location of the jet axis. There is still a small error with maximum amplitude at the jet axis.

REAL PERTURBATION RUN (RPR) EXPERIMENTS

a) J_7 - Experiment

In this experiment we have taken the mean fields of the 55 year run of the first ASR Experiment, zonally averaged them and repeated the same run for 22 years with the "real" perturbations, e.g.,

$$\psi' = \psi - <\overline{\psi}> \qquad (26)$$

where $< . >$ indicates a zonal average. Eq. (5) is used to compute the EPE balance with J_7 as the Jacobian. Again we monitored the EPE balance after 11 and 22 years of integration and the terms did not change significantly. The EPE balance for this experiment is shown in Fig. 3. The dissipation and production terms are almost identical to the first ASR experiment, but now the mean advection and the redistribution of EPE are huge contributors to the balance. Remarkably the error is very small. The analytical solution dictates that the mean advection term has to vanish, which is not the case in this experiment. We discriminated against round-off errors using different methods to damp the leap-frog noise, which results in different instantaneous realizations of the flow. However, the EPE balance did not change by more than one percent. Fig. 4 shows the contributions of the single Jacobians J_1, J_2 and J_3 to J_7 in the EPE balance (before dividing by the factor 3).

The main outstanding single contribution in the mean advection term comes from J_2.

b) J_9 - Experiment

In this experiment we have again taken the 55 year mean fields from the first ASR run, zonally averaged them and repeated the run for 22 years using J_9 for the time integration and diagnosed the EPE

balance using eq. (5) Fig. 5 shows the EPE balance after 22 years and Fig. 6 gives the contributions of all Jacobians involved.

The mean advection term and the error are negligible (as they should be) and the interesting aspect of the EPE balance is again the local minimum in the dissipation term and the huge variation of the different second order Jacobians in the redistribution term (see Fig. 6b). The maxima of all terms in the EPE balance are slightly higher than in the comparable ASR experiment. We do not know if this run without zonally averaged mean fields would produce a comparable error in the EPE balance as in the second ASR experiment.

To our relief, the momentum balance in this experiment does not differ from the momentum balance for case FB in Wolff et al., (1991). This is also true for the energy balance (not shown).

SUMMARY AND CONCLUSION

It has been demonstrated by various authors that the numerical formulation of the advection term with J_7 (Arakawa and Lamb, 1977) is sufficient to compute low order statistics like the momentum and energy budgets in quasi-geostrophic channel models. However, higher order statistics like the eddy potential enstrophy can not be computed accurately due to artificial space and/or time correlations introduced by the J_7 discretization. A fourth order accurate Jacobian operator is required to correctly compute the eddy potential enstrophy (EPE) balance in the quasi-geostrophic channel experiments. Using the accumulated statistics method requires very long time integrations to decrease slight deviations of the mean fields from their zonal average.

ACKNOWLEDGEMENTS

Support for computations was provided by the CSIRO Division of Information Technology Supercomputer Facility.

REFERENCES

ARAKAWA, A., 1966: Computational design for long-term numerical integration of the equations of fluid motion: Two-dimensional incompressible flow. Part I. *J. Comput. Phys.*, **1**, 119–143.

ARAKAWA, A. and LAMB, V.R., (1977): "Computational design of the basic dynamical processes of the UCLA general circulation model", *Meth. Comput. Phys.*, **17**, 173–265.

IVCHENKO, V.O., 1985: On the parametrization of the eddy flows of geostrophic potential vorticity in zonal ocean currents. Izvestiya, *Atmos. Oc. Phys.*, **21**, 660–664.

MARSHALL, J., 1981: On the parametrization of geostrophic eddies in the ocean. *J. Phys. Oceanogr.*, **11**, 257–271.

MARSHALL, J., and SHUTTS, G., 1981: A note on rotational and divergent eddy fluxes. *Journ. Phys. Oceanogr.*, **11**, 1677–1680.

McWILLIAMS, J.C., HOLLAND, W.R., and CHOW, J.H.S., 1978: A description of numerical Antarctic Circumpolar Currents. *Dyn. Atmos. Oceans*, **2**, 213–291.

McWILLIAMS, J.C., and CHOW, J.H.S., 1981: Equilibrium geostrophic turbulence I: A reference solution in a beta-plane channel. *J. Phys. Oceanogr.*, **11**, 921–949.

TREGUIER, A.M., and McWILLIAMS, J.C., 1990: Topographic influences on wind–driven, stratified flow in a β–plane channel: an idealized model for the Antarctic Circumpolar Current. *J. Phys. Oceanogr.*, **20**, 321–343.

WOLFF, J.–O., 1993: QG-CHANNEL – A two–layer quasi–geostrophic channel model, ANTARCTIC CRC Version, Cycle 1. Technical report, in preparation.

WOLFF, J.–O., MAIER–REIMER, E., and OLBERS, D.J., 1991: Wind–driven flow over topography in a zonal β–plane channel: A quasi-geostrophic model of the Antarctic Circumpolar Current. *J. Phys. Oceanogr.*, **21**, 236–264.

WOLFF, J.–O., IVCHENKO, V.O., RICHARDS, K.J., SINHA, B., KLEPIKOV, A.V., OLBERS, D.J., and HENSE, A., 1993: On the parametrization of eddy–fluxes of potential vorticity in flat bottom channel flows, in preparation.

APPLYING THE "MERIDIONAL STREAMFUNCTION" VISUALIZATION TECHNIQUE TO OPEN OCEAN DOMAINS

Eric Deleersnijder and Jean-Marie Beckers

ABSTRACT

It is common practice to represent by a streamfunction the transport field ensuing from the integration – over one horizontal coordinate – of the velocity field predicted by ocean models. This very useful visualization technique requires that the transport field be divergenceless. If this is not the case, it is suggested to extract the divergenceless transport field that is closest to that stemming from the model while verifying the impermeability conditions of the ocean surface and bottom. A variational approach is examined.

1. INTRODUCTION

Most of the quantities computed by ocean models are four-dimensional, i.e., they depend on time and three space coordinates. Since the vast majority of graphical tools are two- or three-dimensional, the graphical representation of the model results requires appropriate mappings onto a two- or three-dimensional space. This may be carried out in numerous ways by means of existing graphical packages.

One must however bear in mind that the role of computer graphics is not just to produce attractive pictures, but to help gain insight into the physics of the ocean flow under study. In other words, physical intuition and reasoning are also needed if profound understanding of the flow's mechanism is sought. Schematically, this might be expressed by the following relation: quality of the interpretation = (physical skill) × (computer graphics skill). This implies, for instance, that the best graphical software will probably prove useless if operated by someone having no idea of ocean dynamics!

An example of an interpretation technique based on little graphical skill but considerable physical skill is the "meridional streamfunction" approach. This technique, which has now become a standard for visualizing and discussing the results of OGCMs (Bryan, 1982; Bryan, 1987; Toggweiler et al., 1989; Killworth et al., 1991; Marotzke and Willebrand, 1991; England, 1992; Semtner and Chervin, 1992), consists in integrating the velocity in meridional planes over the longitudinal width of the ocean basin under study. Assuming that there is no water flux across the land-sea boundaries, the resulting two-dimensional vector field is divergenceless, implying that it may be represented with the help of a streamfunction – termed "meridional streamfunction" since the longitudinal velocity component is ignored. Contours of the streamfunction are drawn, and the difference between the streamfunction values associated with two given isolines corresponds to the water flux flowing between these isolines.

Of course, if it is preferable to integrate over the latitudinal width of the domain, a procedure similar to that described above may be utilized. In fact, the direction of integration does not matter. But, for the vector field to be properly represented by means of a streamfunction, it is crucial that it be divergenceless, meaning that the water velocity normal to the lateral boundaries of the domain of interest must be zero. Here, the "lateral boundaries" are defined to be the surfaces corresponding to the upper and lower values of the space variable over which the flow is integrated.

Thus, when the lateral boundaries are not impermeable, representing the integrated flow with the help of a streamfunction is, in general, impossible. This serious drawback may however be circumvented by resorting to the approximate technique established in the present note.

This study concentrates on the mathematical formulation of the method, leaving actual applications to a forthcoming, more extensive article.

Below, the following vocabulary is utilized: a quantity being measured in m s^{-1} is called "velocity", a "transport" is expressed in m^2 s^{-1} and m^3 s^{-1} (or, equivalently, Sverdrups) are used for "fluxes".

2. VARIATIONAL APPROACH

Consider the domain D depicted in Fig. 7. Let the "lateral coordinate" be $y - y_-(x) \leq y \leq y_+(x)$, which means that the flow in the (x, z) plane is to be represented. The vertical coordinate z is zero at the ocean surface, assumed flat, and is equal to $h(x, y)$ (≥ 0) at the bottom. The model velocity components along the (x, z) axes are (u^*, w^*), w^* being positive in the case of downwelling. The unit vectors ($\mathbf{e}_x$, $\mathbf{e}_y$, $\mathbf{e}_z$) are associated with the (x, y, z) coordinates.

The transport

$$\mathbf{U}^*(x,z) = U^* \mathbf{e}_x + W^* \mathbf{e}_z = \int_{y_-(x)}^{y_+(x)} (u^* \mathbf{e}_x + w^* \mathbf{e}_z)\, dy \qquad (1)$$

is defined in the domain Ω, i.e., $x_- \leq x \leq x_+$ and

$$0 \leq z \leq H(x) \equiv \max_{y_- \leq y \leq y_+} h(x, y)$$

(Fig. 8). The vector field above obeys the following mass conservation equation

$$\frac{\partial U^*}{\partial x} + \frac{\partial W^*}{\partial z} = q^*, \qquad (2)$$

where q^* is the sum of the normal components of the horizontal velocity entering D at (x, y_-) and (x, y_+).

When q^* is zero, $\mathbf{U}^*$ is divergence-free. Hence, this transport may be represented by means of a streamfunction, which is no longer possible when $q^* \neq 0$. In this case, only an appropriate divergenceless part of $\mathbf{U}^*$, hereafter denoted $\mathbf{U}$, may be represented by a streamfunction Ψ, i.e., (Fig. 8)

$$\begin{aligned} \mathbf{U} \;&=\; U\,\mathbf{e}_x \;+\; W\,\mathbf{e}_z \;= \\ \frac{\partial \Psi}{\partial z}\,\mathbf{e}_x \;&-\; \frac{\partial \Psi}{\partial x}\,\mathbf{e}_z \;=\; -\,\nabla \times \Psi\,\mathbf{e}_y, \end{aligned} \tag{3}$$

with $\nabla = \mathbf{e}_x\,\partial/\partial x + \mathbf{e}_z\,\partial/\partial z$. The transport field $\mathbf{U}$ identically satisfies the mass conservation equation $\nabla \bullet \mathbf{U} = 0$. It remains to define what is meant by "an appropriate divergenceless part of $\mathbf{U}^*$".

It seems quite natural to compute $\mathbf{U}$ as the divergence-free transport field that is closest to $\mathbf{U}^*$. Thus, $\mathbf{U}$ may be obtained as the vector field corresponding to the minimum of the functional

$$I \;=\; \int_\Omega \;|\,\mathbf{U} - \mathbf{U}^*\,|^2 \;\,d\Omega\,, \tag{4}$$

with $d\Omega = dx\;dz$.

Many other functionals would have been equally valid, but we opted for a quadratic form, because determining the function rendering such a functional minimum is usually straightforward.

To allow meaningful physical interpretations, it is clear that $\mathbf{U}$ must respect the impermeability of the upper and lower boundaries of Ω. In other words, it is required that Ψ satisfy the following essential conditions:

$$\begin{aligned} [\;\Psi(x, z=0),\;\Psi(x, z=H)\;] \\ =\;(0, \Psi_b = const.), \end{aligned} \tag{5}$$

where Ψ_b represents the constant, horizontal flux flowing through the domain from x_- to x_+.

By expressing that the first order variation of I must be zero, the Euler-Lagrange equations of the minimum principle are obtained, i.e.,

$$\nabla^2\,\Psi \;=\; \frac{\partial U^*}{\partial z} \;-\; \frac{\partial W^*}{\partial x}\,,\;\text{in}\;\Omega\,, \tag{6}$$

$$\begin{aligned} \{\,[\frac{\partial \Psi}{\partial x}]_{x=x_-}\,,\,[\frac{\partial \Psi}{\partial x}]_{x=x_+}\} \\ =\;-\,[\;W(x_-, z),\;W(x_+, z)\;] \\ =\;-\,[\;W^*(x_-, z), W^*(x_+, z)\;]\,\cdot \end{aligned} \tag{7}$$

Since $\nabla^2\,\Psi = \partial U/\partial z - \partial W/\partial x$, Eq. (6) means that $\mathbf{U}$ and $\mathbf{U}^*$ must have the same "vorticity". The boundary conditions (7) appear as "natural conditions" of the minimum principle, while the impermeability of the surface and the bottom are imposed as "essential conditions" (Fig. 8).

Relations (5) – (7) form a well-posed, elliptic, partial differential problem, the solution of which is easily obtained. However, Ψ_b is unkwown. In fact, Ψ_b must be such that I be minimum.

The value of Ψ_b might be determined by a "brute force", iterative method. Let k represent an integer index associated with the iterations. If I_k, I_{k+1} and I_{k+2} denote successive values of I corresponding to $\Psi_{b,k}$, $\Psi_{b,k+1}$ and $\Psi_{b,k+2}$, respectively, it is possible to obtain an approximation to the value of Ψ_b rendering I minimum. Indeed, assuming that I may be quadratically interpolated over $\Psi_{b,k}$, $\Psi_{b,k+1}$ and $\Psi_{b,k+2}$, expressing that $\partial I/\partial \Psi_b = 0$, one gets

$$\Psi_{b,k+3} \;=\; -\,\frac{A}{2B}\,,$$

where

$$\begin{aligned} A = (I_{k+1} - I_k)(\Psi^2_{b,k+2} - \Psi^2_{b,k+1}) \;- \\ (I_{k+2} - I_{k+1})(\Psi^2_{b,k+1} - \Psi^2_{b,k}) \\ B = (I_{k+2} - I_{k+1})(\Psi_{b,k+1} \;-\; \Psi_{b,k}) \;- \\ (I_{k+1} - I_k)(\Psi_{b,k+2} - \Psi_{b,k+1})\cdot \end{aligned} \tag{8}$$

This process may be repeated until the minimum of I is sufficiently approached.

Another iterative method may be equally valid for seeking the minimum of I over Ψ_b. Whatever the method selected, it will be necessary to solve the problem (5) – (7) several times. This may be computationally expensive, especially if the number of grid points placed in Ω is large.

Fortunately, by somewhat reworking the partial differential problem (5) – (7), it may be seen that a direct, non-iterative determination of Ψ_b is possible.

3. NON-ITERATIVE METHOD

As the problem to be solved is linear, its solution may be considered a linear combination of several functions, i.e.,

$$\Psi(x, y) \;=\; \Psi^0(x, y) \;+\; \Psi_b \Psi^1(x, y)\,\cdot \tag{9}$$

The function Ψ^0 is the solution of (5) – (7), except that

$$\Psi^0(x, z=H) \;=\; 0\,, \tag{10}$$

which means that no water flux through the domain is associated with Ψ^0. On the other hand, Ψ^1 is obtained from the following partial differential problem:

$$\nabla^2\,\Psi^1 \;=\; 0,\;\text{in}\;\Omega\,, \tag{11}$$

$$[\;\Psi^1(x, z=0),\;\Psi^1(x, z=H)\;] \;=\; (0, 1)\,, \tag{12}$$

$$\{ [\frac{\partial \Psi^1}{\partial x}]_{x=x_-} , [\frac{\partial \Psi^1}{\partial x}]_{x=x_+} \} = (0, 0) \cdot \quad (13)$$

For a given domain Ω, Ψ^1 is independent of the flow regime. Thus, Ψ^1 should be calculated once and for all.

It is easily seen that $\Psi^0 + \Psi_b \Psi^1$ is actually the solution to (5) – (7). To determine Ψ_b, we introduce (9) into (4) and seek the minimum of I over Ψ_b. Accordingly, Ψ_b is the solution of $\partial I / \partial \Psi_b = 0$, i.e.,

$$\Psi_b = - \frac{\int_\Omega (\nabla \Psi^0 \bullet \nabla \Psi^1 + \mathbf{e}_y \bullet (\mathbf{U}^* \times \nabla \Psi^1)) \, d\Omega}{\int_\Omega | \nabla \Psi^1 |^2 \, d\Omega} \quad (14)$$

which indeed corresponds to the minimum of I, because

$$\frac{\partial^2 I}{\partial \Psi_b^2} = \int_\Omega | \nabla \Psi^1 |^2 \, d\Omega \geq 0 \cdot \quad (15)$$

4. CONCLUSION

The mathematical foundations of a technique aiming at adapting the classical "meridional streamfunction" method to open ocean domains has been discussed. It must be stressed that the approach suggested in the present note does not simply amount to taking the rotational part of a given two-dimensional transport field: the transport field we determine is divergenceless and has the same curl as that produced by the model, but, in addition, it is required that it satisfy the impermeability of the upper and lower boundaries of the domain.

Whether or not the technique discussed here will turn out to be useful is presently not clear. It has yet to be applied to model results, which will then allow assessing the physical interpretations it will lead to. It is however believed that our method will prove appropriate for visualizing the results of large- and small-scale ocean models, as well as those of atmospheric models – after minor modifications.

Finally, it must be stressed that determining Ψ only is not sufficient, since it does not permit us to evaluate to what extent $\mathbf{U}$ is a good approximation of the modelled transport field $\mathbf{U}^*$. As a result, it will be necessary to systematically estimate the "distance" between $\mathbf{U}$ and $\mathbf{U}^*$, for example, by computing

$$\varepsilon = [\frac{\int_\Omega | \mathbf{U} - \mathbf{U}^* |^2 \, d\Omega}{\int_\Omega | \mathbf{U}^* |^2 \, d\Omega}]^{\frac{1}{2}} \cdot \quad (16)$$

Clearly, for large ε, the greatest precaution will be required when discussing the field $\mathbf{U}-$ or Ψ. In such a case, it might turn out preferable to modify the domain of integration D so as to obtain a smaller value of ε, allowing more relevant discussion of the resulting streamfunction Ψ.

REFERENCES

BRYAN, F., 1987: Parameter sensitivity of primitive equations ocean general circulation models. *J. Phys. Oceanogr.*, **17**, 970–985.

BRYAN, K., 1982: Seasonal variation in meridional overturning and poleward heat transport in the Atlantic and Pacific oceans: a model study. *J. Mar. Res.*, **40**, 39–53.

ENGLAND, M.H., 1992: On the formation of Antarctic Intermediate and Bottom Water in ocean general circulation models. *J. Phys. Oceanogr.*, **22**, 918–926.

KILLWORTH, P.D., STAINFORTH, D., WEBB, D., and PATERSON, S.M., 1991: The development of a free-surface Bryan-Cox-Semtner ocean model. *J. Phys. Oceanogr.*, **21**, 1333–1348.

MAROTZKE, J., and WILLEBRAND, 1991: Multiple equilibria of the global thermohaline circulation. *J. Phys. Oceanogr.*, **21**, 1372–1385.

SEMTNER, A.J., and CHERVIN, R.M., 1992: Ocean general circulation from a global eddy-resolving model. *J. Geophys. Res.*, **97**, 5493–5550.

TOGGWEILER, J.R., DIXON, K., and BRYAN, K., 1989: Simulation of radiocarbon in a coarse-resolution world ocean model, 2. Distributions of bomb-produced carbon 14. *J. Geophys. Res.*, **94**, 8243–8264.

A FAST AND COMPLETE CONVECTION SCHEME FOR OCEAN MODELS

S. Rahmstorf

Imagine having three half-filled glasses of wine lined up in front of you. On the left a German Riesling, in the middle a French Burgundy and on the right a Chardonnay from New Zealand. Imagine further that you're not much of a connoisseur, so you want to mix the three together to a refreshing drink, with exactly the same mixture in each glass. The trouble is, you can only mix the contents of two adjacent glasses at a time. So you start off by mixing the Riesling with the Burgundy, then you mix this mixture with the Chardonnay, then... How often do you need to repeat this process until you get an identical mix in all glasses?

Incidentally, putting this question to a friend is a good test to see whether she (or he) is a mathematician or a physicist. A mathematician would answer "an infinite number of times", while a physicist would be well aware that there is only a finite number of molecules involved, so you can get your perfect drink with a finite mixing effort (only you would have no way to tell whether you've got it or not).

In any case, the number of times you need to mix is very large, and this is the problem of the standard convection scheme of the GFDL ocean model (Cox 1984), which mixes two adjacent levels of the water column if they are statically unstable. The model includes the option to repeat this mixing process a number of times at each time step, as an iteration process towards complete removal of static instabilities. The minimum number of iterations needed to mix *some* of the information from layer 1 down to layer n is $n-1$.

To avoid this problem, one needs to relax the condition that only two levels may be mixed at a time. To achieve complete mixing, a convection scheme is required that can mix the whole unstable part of the water column in one go. I have been using such a scheme back in 1983 in a one-dimensional mixing model for the Irish Sea, and I'm sure many other people have been using similar ones. Marotzke (1991) introduced such a scheme into the GFDL ocean model. It appears that it hasn't been taken up as enthusiastically as it might have been, and an implicit convection scheme (which increases the vertical diffusivity at unstable parts of the water column) has been preferred because of lower computational cost (e.g. Weaver et al., 1993). However, it is not difficult to set up a complete convection scheme which uses less computer time than the implicit scheme.

THE STANDARD SCHEME

Since the GFDL model works the grid row by row, we'll only discuss how one grid-row is treated. Here's how:

(1) Compute the densities for all grid cells in the row. Two adjacent levels are always referenced to the same pressure in order to get the static stability of this pair of levels.
(2) Mix all unstable pairs.
(3) Since we have now only compared and mixed "even" pairs (i.e. levels 1 & 2; levels 3 & 4; etc), repeat steps (1) and (2) for "odd" pairs (i.e. levels 2 & 3; levels 4 & 5; etc).
(4) Repeat steps (1)–(3) a predetermined number of times.

There are a couple of problems here. We've already said that strictly speaking this never leads to complete mixing of an unstable water column. So the process is repeated several times at each time step to approximate complete mixing. But each time *all* grid cells are checked for instabilities again, even those we already found to be stable. Each density calculation requires evaluation of a third order polynomial in T and S. This is where the cpu time is eaten up.

MAROTZKE'S SCHEME

This scheme works as follows:

(1) Same as step (1) above, except that the stability of *all* pairs of grid cells is checked, odd and even pairs (so that the density of interior levels is computed twice, for two different reference pressures).
(2) Don't mix yet: just mark all unstable pairs and find continuous regions of the water column which are unstable (neutral stability is treated as unstable).
(3) Mix the unstable regions.
(4) If there was instability in any column, repeat steps (1) to (3). Those columns which were completely stable in the previous round are not dealt with again in (2) and (3), but the densities are still recomputed for the entire grid row. Repeat until no more instabilities are found.

So Marotzke relaxed the condition that only two levels are mixed at a time, and complete mixing will be achieved with at most $k-1$ passes through the water column, if k is the number of model levels. However, if only one grid point of a row requires n iterations, the densities for the entire grid row will be recomputed n times, so it still doesn't look too good in terms of cpu efficiency.

THE FAST WAY

(1) Compute all densities like in (1) of Marotzke.

(2) Compare all density pairs to find instabilities.

From here on, deal column by column with those grid points where an instability was found, performing the following steps:

(3) Mix the uppermost unstable pair.
(4) Check the next level below. If it is less dense than the mixture, mix all three. Continue incorporating more levels in this way, until a statically stable level is reached.
(5) Then check the level *above* the newly mixed part of the water column, to see whether this has become unstable now. If so, include it in the mixed part and go back to (3). If not, search for more unstable regions below the one we just mixed, by working your way down the water column comparing pairs of levels; if you find another unstable pair, go to (3).

Note that levels which have been mixed are from then on treated as a unit. This scheme has a slightly more complicated logical structure; it needs a few more integer variables and *if* statements to keep track of which part of the water column we have already dealt with. The advantage is that we only recompute the densities of those levels we need; levels which are not affected by the convection process are only checked once. The scheme includes diagnostics which allow to plot the convection depth at each grid point.

DISCUSSION

Perhaps these schemes are best discussed with an example. Imagine a model with five levels. At one grid point levels 2 & 3 and levels 3 & 4 are statically unstable. The standard scheme will, at the first pass, mix 3 & 4 and then 2 & 3. It will repeat this *ncon* times. Marotzke's scheme will mark the unstable pairs and then mix 2–4 in one go. It will then return to this column for a second pass and check all levels once more. My scheme will mix 2 & 3; then compare the densities of 3 & 4 and (if unstable) mix 2–4 like Marotzke's scheme. It will then recompute the density of level 4, compare levels 4 & 5 and mix 2–5 if unstable. Finally it will compare 1 & 2 again, since the density of 2 has changed in the mixing process, so level 1 might have become statically unstable. Only the density of 2 is recalculated for this.

Note that Marotzke's scheme handles the initial mixing of levels 2–4 more efficiently. Probably my scheme could be made slightly faster still by including the "marking" feature from Marotzke's scheme (the schemes were developed independently). However, in the typical convection situation only levels 1 & 2 are initially unstable, due to surface cooling. In this situation marking doesn't help. My scheme saves time by "remembering" which parts of the water column we already know to be stable, and rechecking only those levels necessary.

There is a subtlety that should be mentioned: due to the non-linear equation of state the task of removing all static instability from the water column may not have a unique solution. In the example above, mixing 2 & 3 could yield a mixture with a lower density than level 4, in spite of 3 being denser than 4, and 2 being denser than 3 originally. In this case, my scheme would only mix 2 & 3, while Marotzke's scheme would still mix 2–4. So both schemes are not strictly equivalent, though for all practical purposes they almost certainly are.

I performed some test runs with the GFDL modular ocean model (MOM) in a two-basin configuration (the same as used by Marotzke and Willebrand 1991). The model has ca. 1000 horizontal grid points and 15 levels, and was integrated for 1 year (time step 1.5 h) on a Cray YMP. Three different model states were used: (A) a state with almost no static instability, achieved by strong uniform surface heating; (B) a state with convection occurring at about 15% of all grid points; (C) a state with convection at 30% of all grid points. The latter two were near equilibrium, with permanent convection. I compared the overall cpu time consumed by these runs with different convection schemes. The standard scheme was tried for three different numbers of iterations *ncon*. The results are summarised in the table; the overall cpu time is given relative to a run with no convection scheme.

Convection scheme	relative cpu time		
	A	B	C
No convection scheme	1	1	1
standard, $ncon = 1$	1.13	1.13	1.13
standard, $ncon = 7$	1.88	1.89	1.92
standard, $ncon = 10$	2.25	2.27	2.32
implicit	1.52	1.52	1.52
complete	1.12	1.20	1.36

I was surprised to find that the few innocent-looking lines of model code that handle the convection consume a large percentage of the overall processing time. The numbers are probably an upper limit; a model with realistic topography and time-dependent forcing will use a bigger chunk of the cpu time for iterations in the relaxation routine for the stream function, so that the *relative* amount spent on convection will be lower. In my test runs, the standard scheme adds 13% cpu time per pass. My complete convection scheme used as much time as 1–3 iterations of the standard scheme, depending on the amount of convection. For zero convection it is as fast as one pass of the standard scheme, because it does the same job in this case. Additional cpu time is only used at those grid

points where convection actually occurs. My scheme is considerably faster than the implicit scheme, especially for models where convection happens only at a few grid points, or only part of the time. I did not have Marotzke's scheme available for the test, but in his 1991 paper he mentions a comparison where the computation time with the implicit scheme was 60% of that with his scheme. This would give Marotzke's scheme a relative cpu time of about 2.5 in the table, with strong dependence on the amount of convective activity.

Surface heat fluxes looked identical in the runs with the implicit and complete schemes. The standard scheme showed significant deviations, however, in the surface flux as well as the convective heat flux at different depths. This is not surprising, since the rate at which heat is brought up by convection will be reduced if mixing is incomplete. The runs with $ncon = 7$ and $ncon = 10$ still differed noticeably from each other, and from the complete mixing case. It is possible that this could affect the deep circulation, which is driven by convective heat loss, but I didn't do long integrations to test this. The problem gets worse for longer time steps; with the standard scheme the rate of vertical mixing depends on the time step length. If acceleration techniques are used ("split time stepping", Bryan 1984), the final equilibrium could differ from one without acceleration due to this unwanted time-step dependence. Marotzke (1991) reports a case where the choice of convective scheme had a decisive influence on the deep circulation. The intention of this note is not to examine these problems any further; it is to provide an efficient alternative.

CONCLUSION

I have described a convection scheme which completely removes static instability from the water column in one pass, and which is much faster than the implicit scheme of the GFDL model. This scheme avoids possible problems resulting from the incomplete mixing in the standard scheme, while only using as much computer time as 1–3 iterations of the standard scheme.

REFERENCES

BRYAN, K., 1984: Accelerating the convergence to equilibrium of ocean-climate models. *Journal of Physical Oceanography*, **14**, 666–673.

COX, M.D., 1984: GFDL Ocean Group Technical Report, 1: A primitive equation, 3-dimensional model of the ocean, *GFDL*, Princeton University, Princeton, 143 pp.

MAROTZKE, J., 1991: Influence of convective adjustment on the stability of the thermohaline circulation. *Journal of Physical Oceanography*, **21**, 903–907.

MAROTZKE, J., and WILLEBRAND, J., 1991: Multiple equilibria of the global thermohaline circulation. *Journal of Physical Oceanography*, **21**, 1372–1385.

WEAVER, A.J., SARACHIK, E.S., and MAROTZKE, J., 1991: Freshwater flux forcing of decadal and interdecadal oceanic variability. *Nature*, **353**, 836–838.

WEAVER, A.J., MAROTZKE, J., CUMMINS, P.F., and SARACHIK, E.S., 1993: Stability and variability of the thermohaline circulation. *Journal of Physical Oceanography*, **23**, 39–60.

Ocean Modelling is edited on behalf of SCOR by Peter Killworth, Michael Davey, Jeff Blundell and typed by Janice Lewis. Support is provided by the U.S. Office of Naval Research. Could contributors please address correspondence to:
"The Editor, Ocean Modelling,
NERC Oceanographic Unit,
Department of Atmospheric, Oceanic and Planetary Physics,
Clarendon Laboratory,
Parks Road,
OXFORD, OX1 3PU".
Please notify us if you change your address.

CONTRIBUTORS

J.-O. Wolff
ANTARCTIC CRC
University of Tasmania
GPO Box 252c
Hobart, TAS 7001
Australia

A.V. Klepikov
Alfred-Wegener-Institut für
Polar- und Meeresforschung
Bremerhaven
Germany

D.J. Olbers
Alfred-Wegener-Institut für
Polar- und Meeresforschung
Bremerhaven
Germany

Vl. N. Stepanov
Institute of Oceanology
Russian Academy of Sciences
Krasikova 23
Moscow 117218
Russia

E. Deleersnijder
Unité ASTR
Institut d'Astronomie et de
Géophysique G. Lemaître
Université Catholique de Louvain
2 Chemin du Cyclotron
B-1348 Louvain-la-Neuve
Belgium

J-M. Beckers
GHER
Institut de Physique
Sart Tilman B5
Université de Liége
Belgium

S. Rahmstorf
Institut für Meereskunde
Düesternbrooker Weg 20
24105 Kiel
Germany

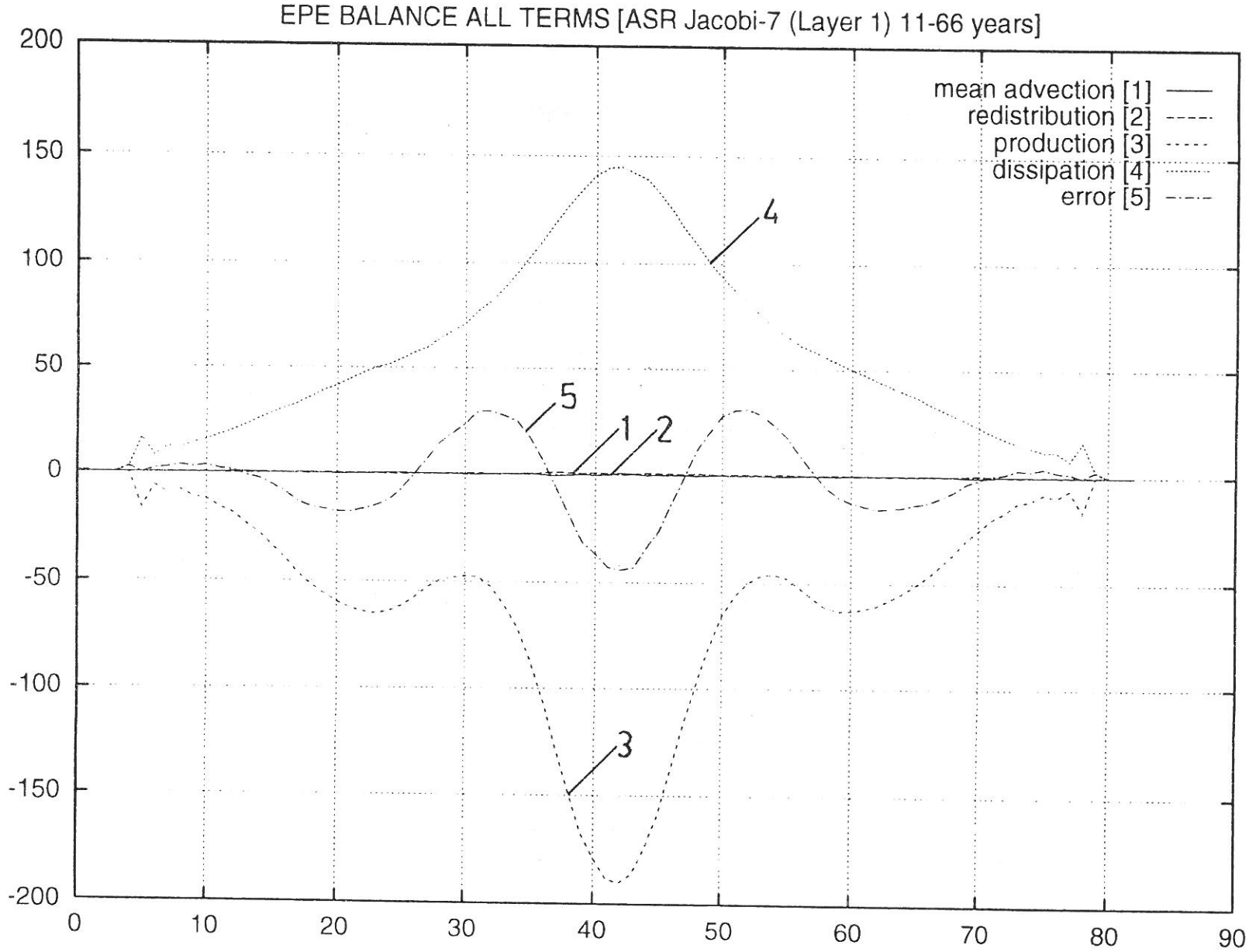

FIGURE 1
(Wolff, Klepikov and Olbers)

Zonally averaged terms in the upper layer EPE balance eq. (6) for the ASR flat bottom experiment using J_7 in the advection routine. Units are $10^{-13}\ m^2 s^{-3}$. The northern boundary of the channel is to the left. The time averaging interval is 55 years.

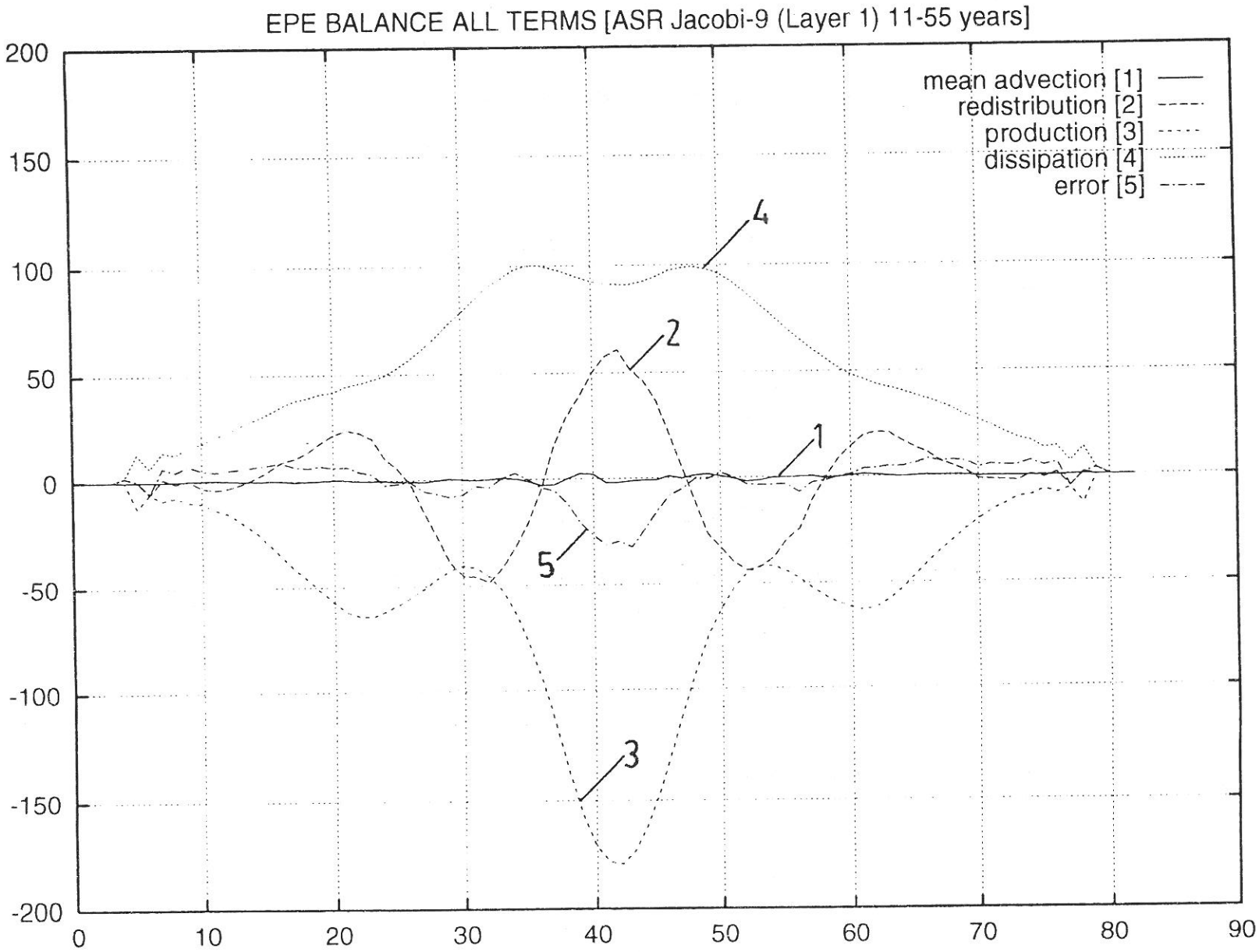

FIGURE 2
(Wolff, Klepikov and Olbers)

Zonally averaged terms in the upper layer EPE balance eq. (6) for the ASR flat bottom experiment using J_9 in the advection routine. Units are $10^{-13}\ m^2 s^{-3}$. The time averaging interval is 44 years.

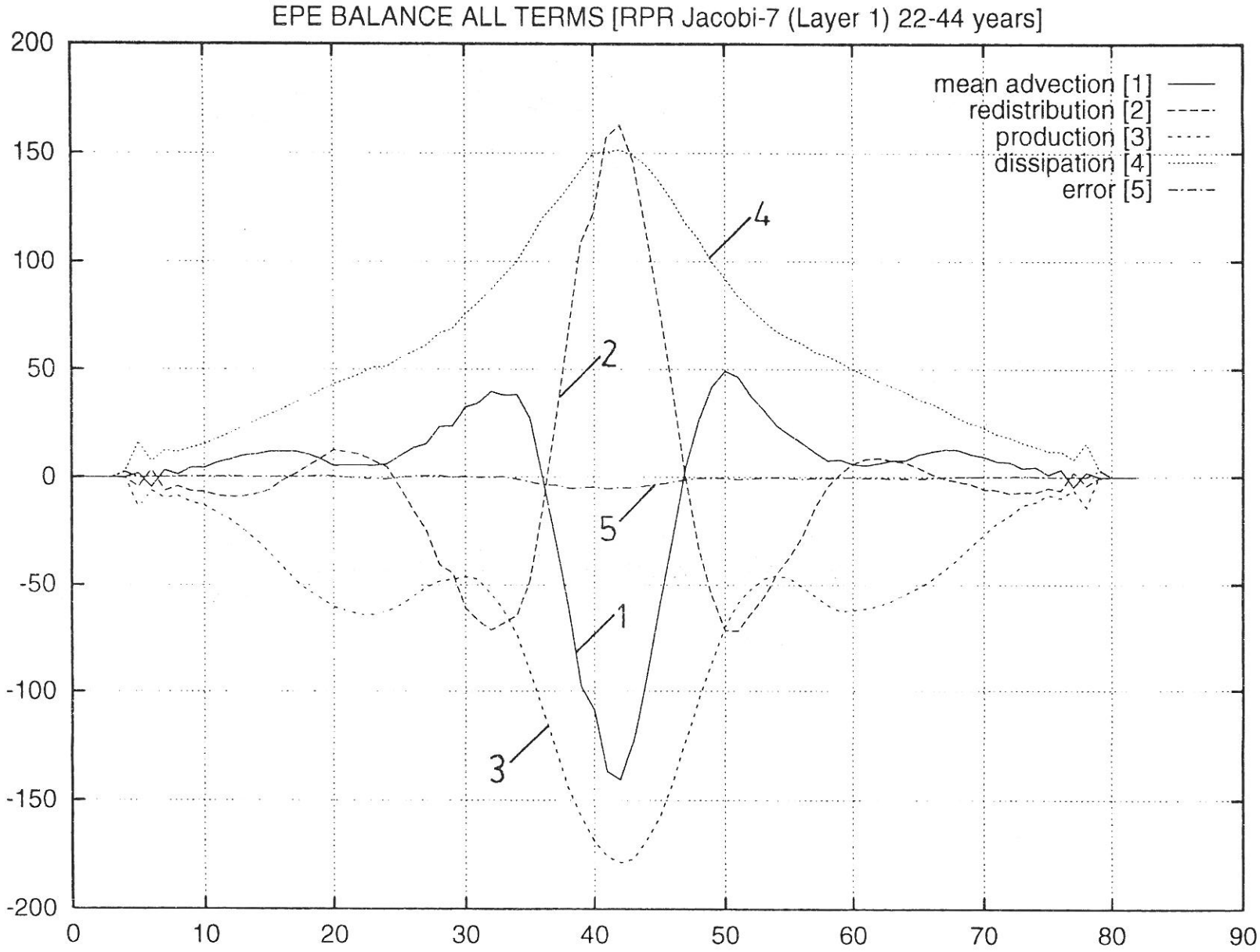

FIGURE 3
(Wolff, Klepikov and Olbers)

Zonally averaged terms in the upper layer EPE balance eq.(5) for the RPR flat bottom experiment using J_7 in the advection routine. Units are 10^{-13} m^2s^{-3}. The time averaging interval is 22 years.

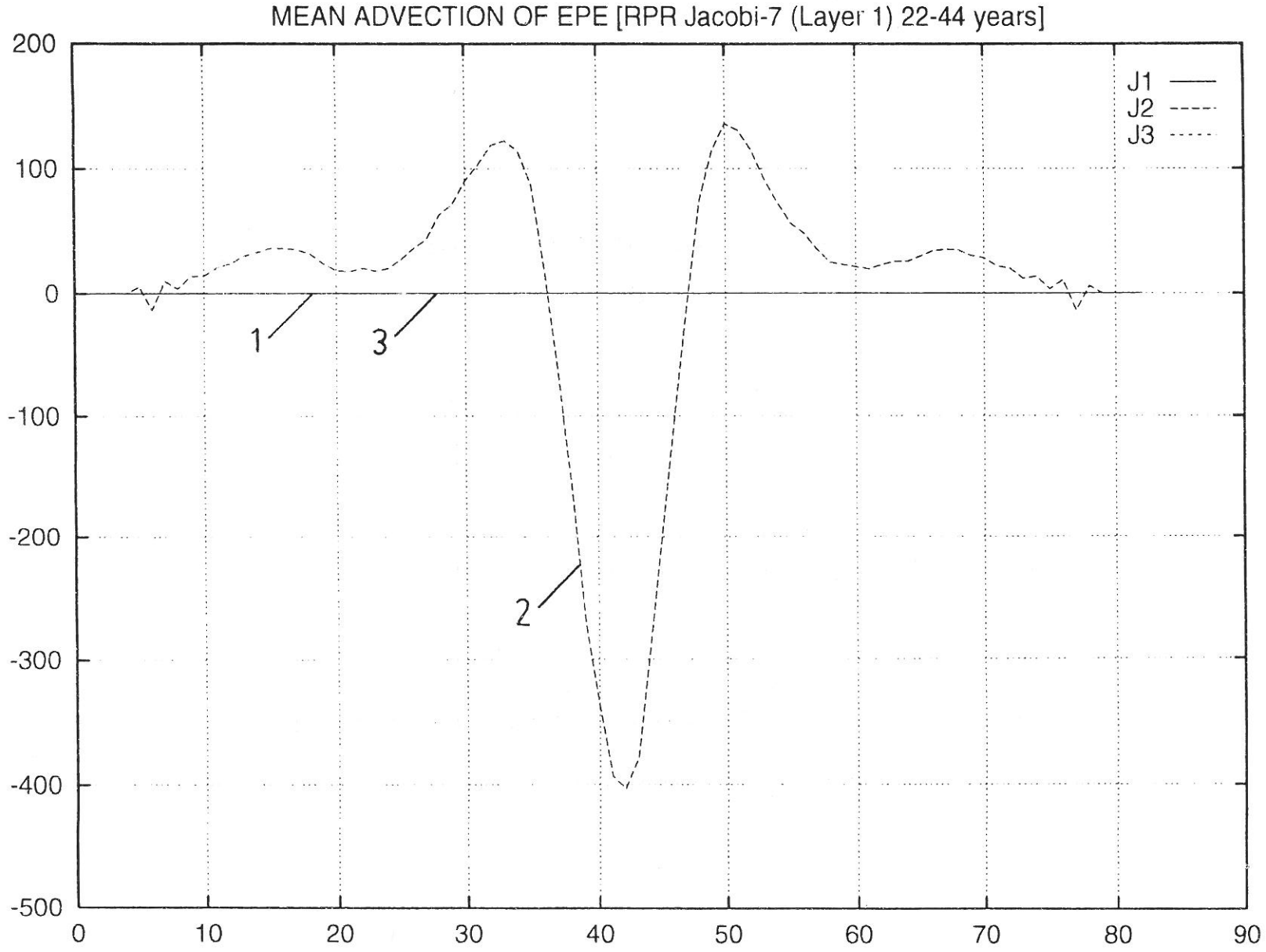

FIGURE 4
(Wolff, Klepikov and Olbers)

Zonally averaged contributions of the discretized Jacobian operators J_1, J_2 and J_3 to the mean advection term in the upper layer EPE balance eq. (5) for the RPR flat bottom experiment using $J_7 = 1/3\,[J_1 + J_2 + J_3]$ in the advection routine. Units are 10^{-13} m^{2}s^{-3}. The time averaging interval is 22 years.

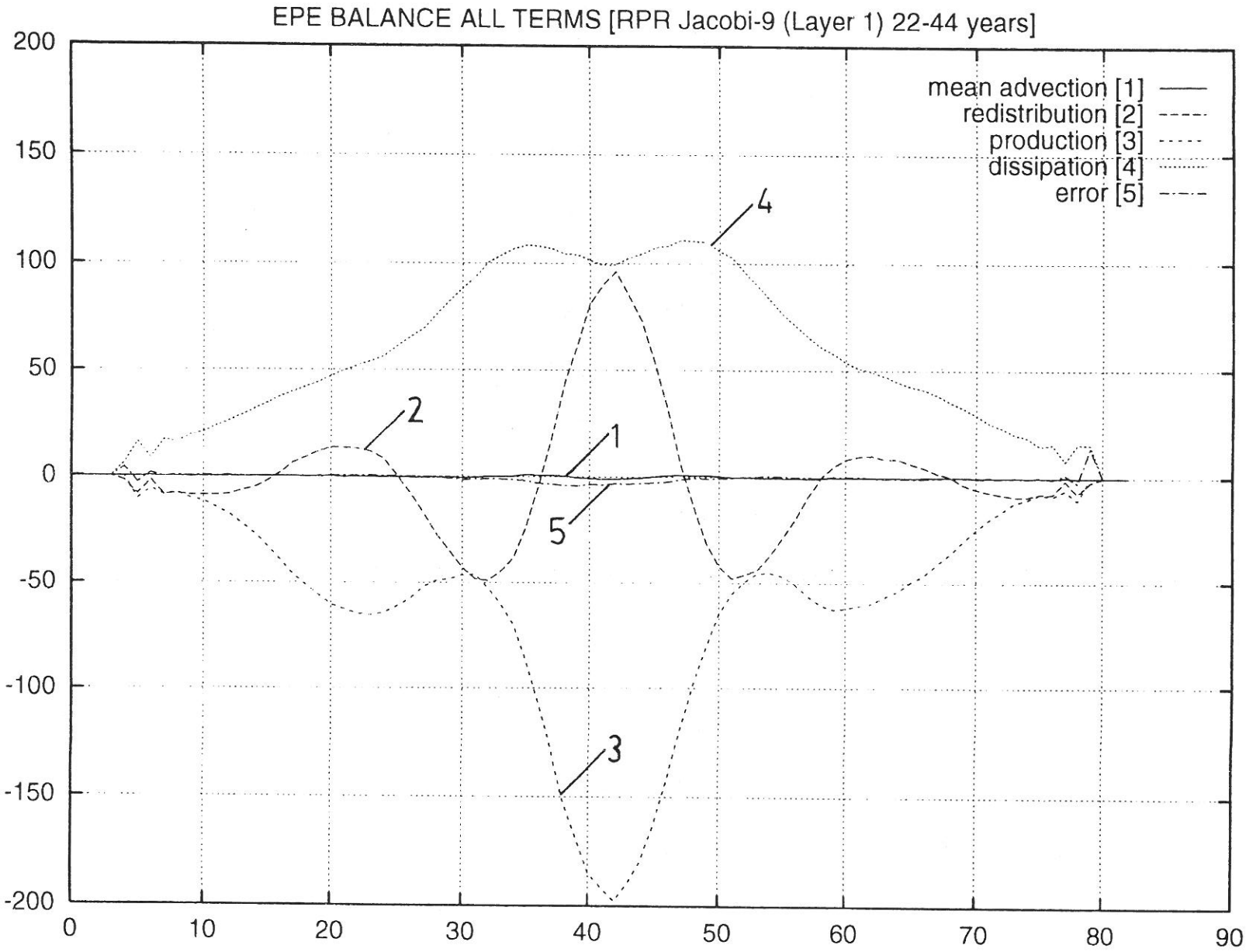

FIGURE 5
(Wolff, Klepikov and Olbers)

Zonally averaged terms in the upper layer EPE balance eq. (5) for the RPR flat bottom experiment using J_9 in the advection routine. Units are $10^{-13}\mathrm{m}^2\mathrm{s}^{-3}$. The time averaging interval is 22 years.

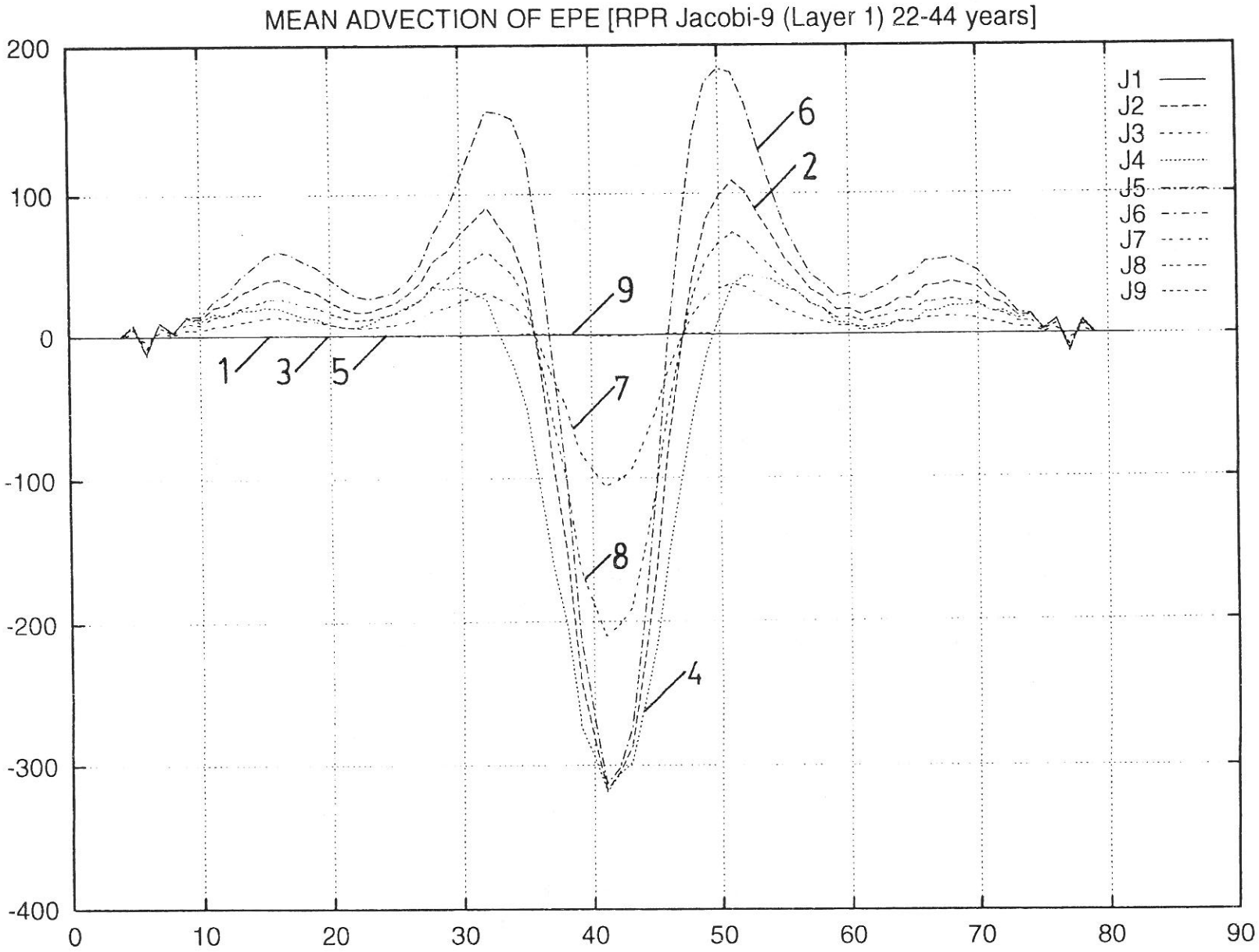

FIGURE 6a
(Wolff, Klepikov and Olbers)

Zonally averaged contributions of the discretized Jacobian operators J_1 to J_9 to the mean advection term in the upper layer EPE balance eq. (5) for the RPR flat bottom experiment using J_9 in the advection routine. Units are 10^{-13} $m^2 s^{-3}$. The time averaging interval is 22 years.

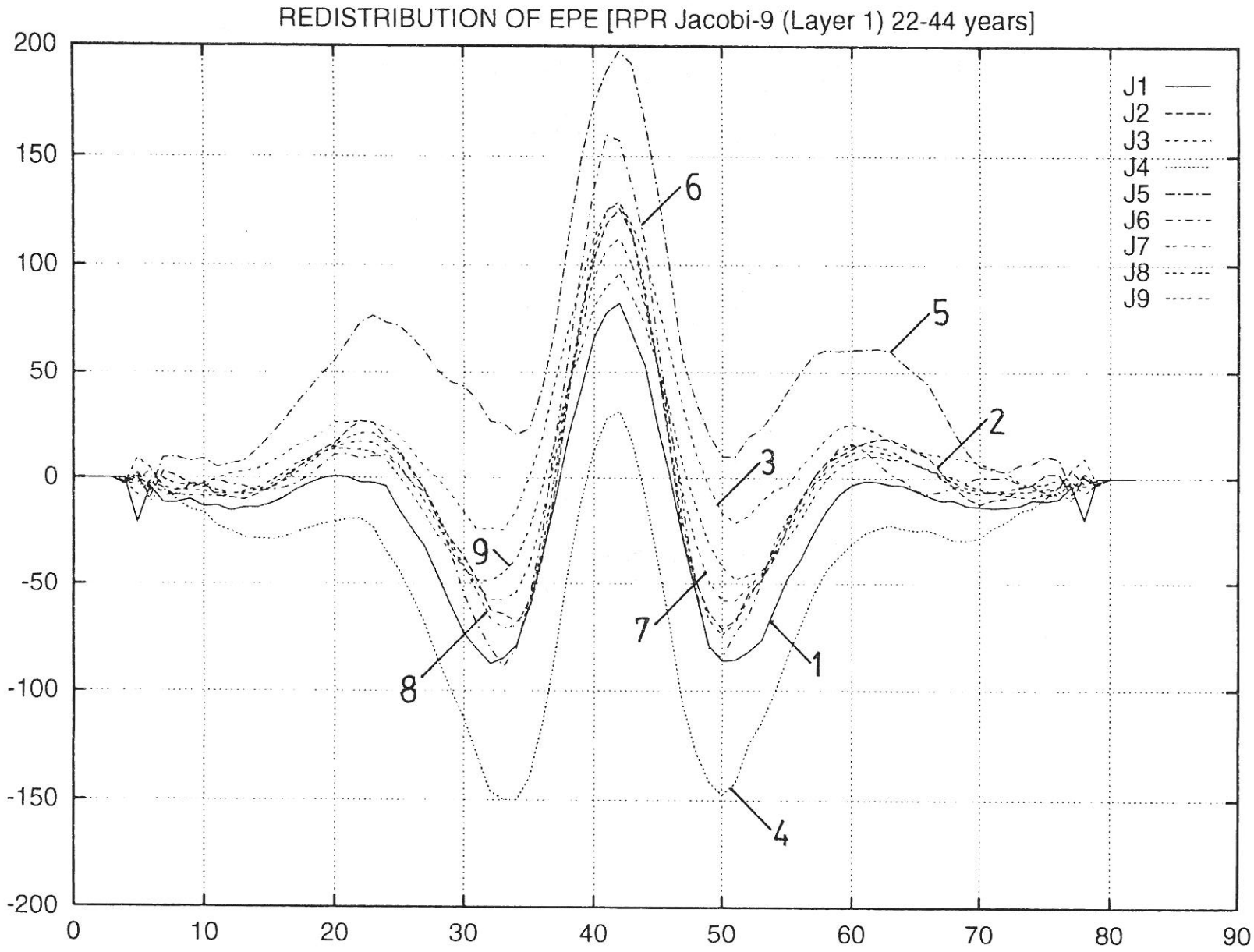

FIGURE 6b
(Wolff, Klepikov and Olbers)
As 6a but for the redistribution of EPE.

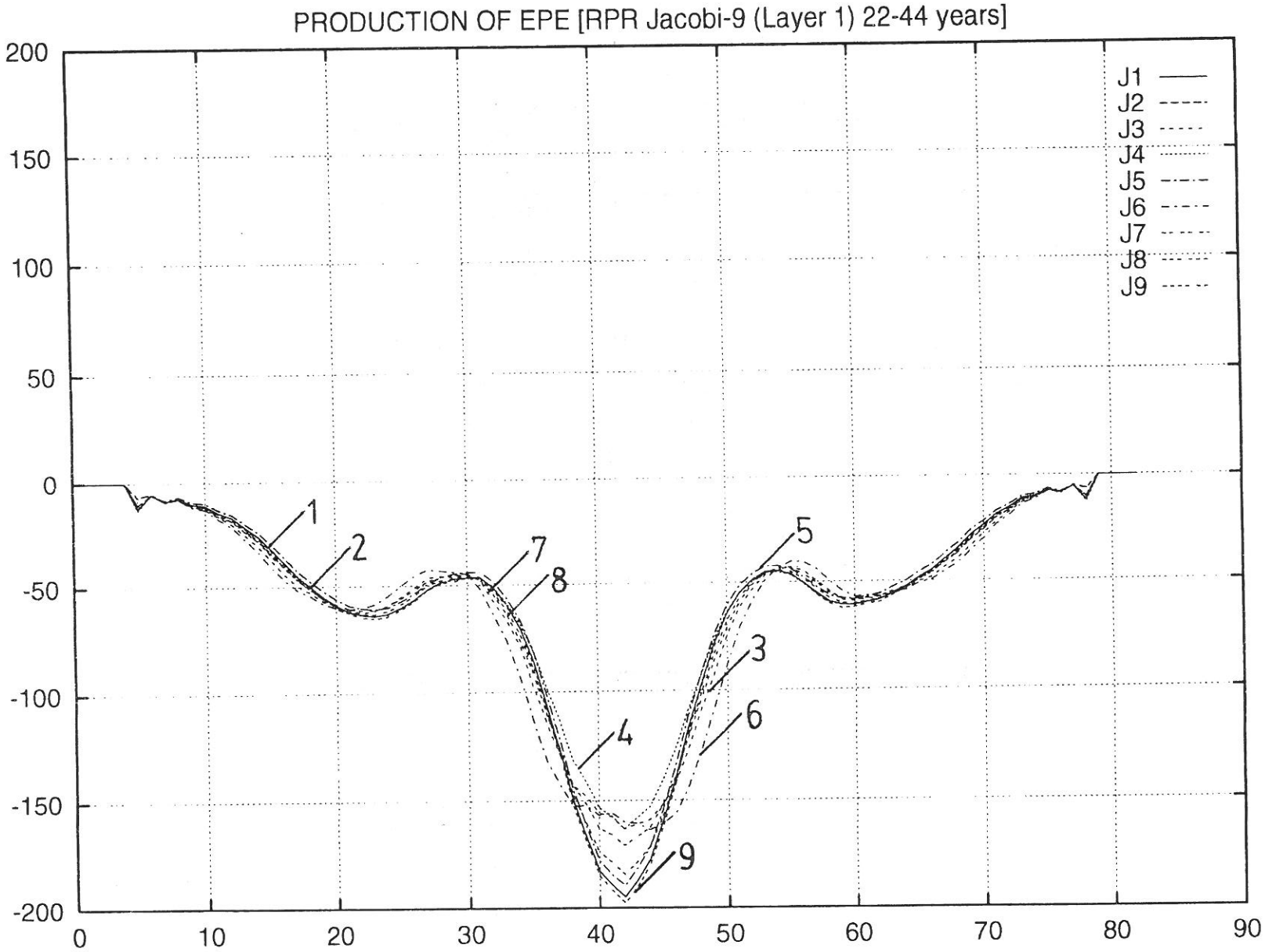

FIGURE 6c
(Wolff, Klepikov and Olbers)
As 6a but for the production of EPE.

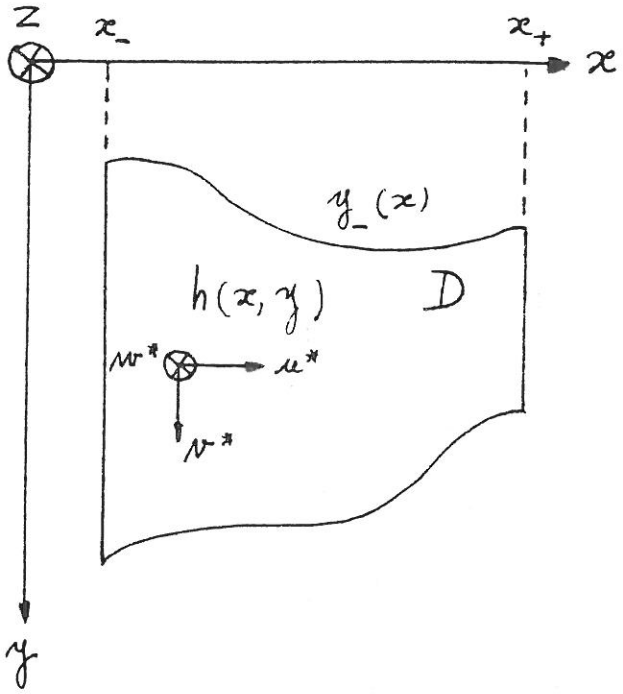

FIGURE 7
(Deleersnijder and Beckers)
The domain of interest D, with the direction of the coordinate axes and the velocity components.

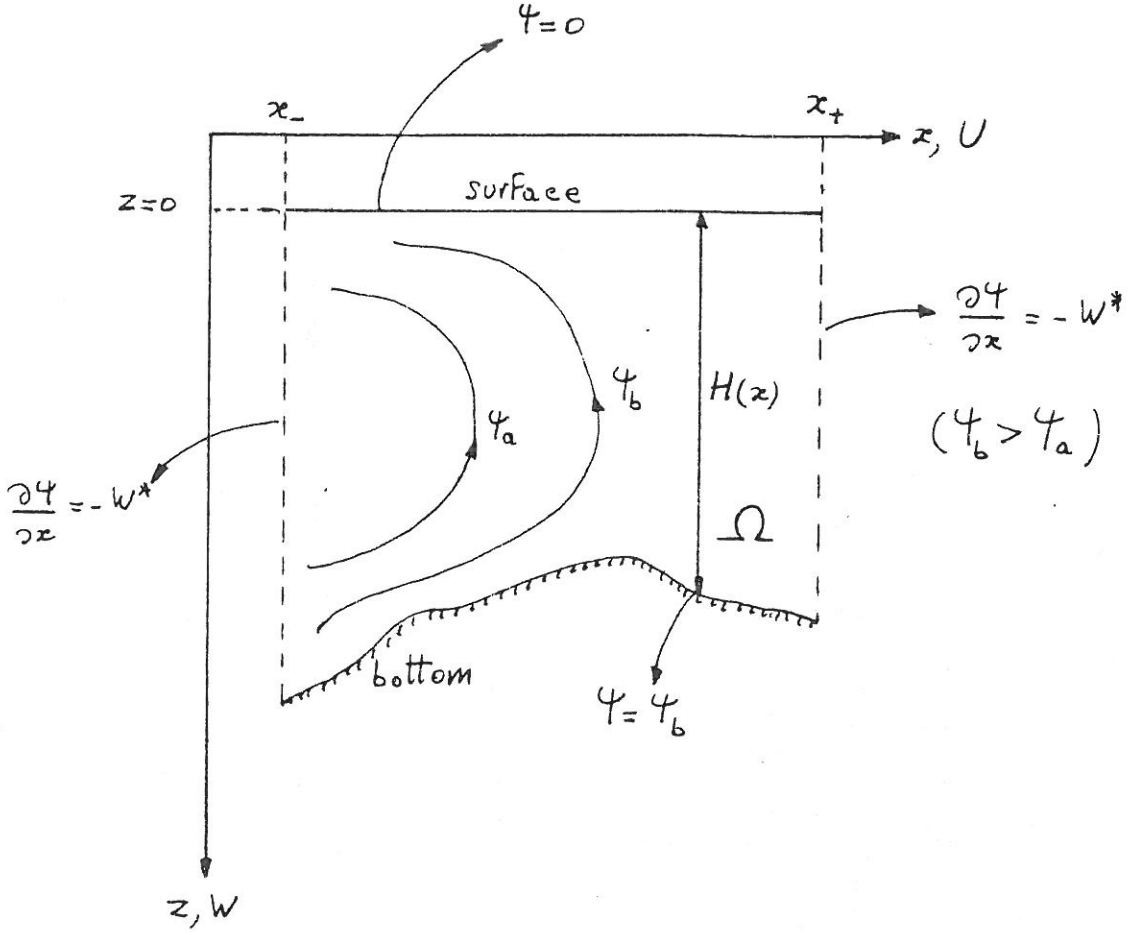

FIGURE 8
(Deleersnijder and Beckers)

The domain Ω in the vertical plane (x, z), with the boundary conditions to be applied to the streamfunction Ψ.